JAMES | Journal of Advances in Modeling Earth Systems

RESEARCH ARTICLE
10.1029/2018MS001478

Prescribing Zonally Asymmetric Ozone Climatologies in Climate Models: Performance Compared to a Chemistry-Climate Model

Cameron D. Rae[1], James Keeble[1,2], Peter Hitchcock[3,4], and John A. Pyle[3]

[1]Centre for Atmospheric Science, Department of Chemistry, University of Cambridge, Cambridge, UK, [2]NCAS, University of Cambridge, Cambridge, UK, [3]Department of Applied Mathematics and Theoretical Physics, University of Cambridge, Cambridge, UK, [4]Now at Earth and Atmospheric Sciences Department, Cornell University, Ithaca, NY, USA

Key Points:
- Dynamical feedbacks resulting from ozone zonal asymmetries are important for accurately representing Northern Hemisphere circulation patterns during wintertime
- Three simulations using different methods of specifying ozone mixing ratios are compared with a fully coupled CCM simulation in order to examine the pathways by which zonal ozone asymmetries influence modeled dynamics
- Dynamical feedbacks occurring in a coupled CCM can be reproduced, at a greatly reduced computational cost, by appropriately placing a prescribed ozone climatology onto a dynamically evolving coordinate

Supporting Information:
- Supporting Information S1
- Figure S1
- Figure S2
- Figure S3

Correspondence to:
C. D. Rae,
camerondrae@gmail.com

Citation:
Rae, C. D., Keeble, J., Hitchcock, P., & Pyle, J. A. (2019). Prescribing zonally asymmetric ozone climatologies in climate models: Performance compared to a chemistry-climate model. *Journal of Advances in Modeling Earth Systems*, *11*, 918–933. https://doi.org/10.1029/2018MS001478

Received 17 AUG 2018
Accepted 19 MAR 2019
Accepted article online 28 MAR 2019
Published online 11 APR 2019

Abstract Three different methods of specifying ozone in an atmosphere-only version of the HadGEM3-A global circulation model are compared to the coupled chemistry configuration of this model. These methods include a specified zonal-mean ozone climatology, a specified 3-D ozone climatology, and a calculated-asymmetry scheme in which a specified zonal-mean ozone field is adapted online to be consistent with dynamically produced zonal asymmetries. These simulations all use identical boundary conditions and, by construction, have the same climatological zonal-mean ozone, that of the coupled chemistry configuration of the model. Prescribing ozone, regardless of scheme, results in a simulation which is 3–4 times faster than the coupled chemistry-climate model (CCM). Prescribing climatological zonal asymmetries leads to a vortex which is the correct intensity but which is systematically displaced over regions with lower prescribed ozone. When zonal asymmetries in ozone are free to evolve interactively with model dynamics, the modeled wintertime stratospheric vortex shape and mean sea level pressure patterns closely resemble that produced by the full CCM in both hemispheres, in terms of statistically significant differences. Further, we separate out the two distinct pathways by which zonal ozone asymmetries influence modeled dynamics. We present this interactive-ozone zonal-asymmetry scheme as an inexpensive tool for accurately modeling the impacts of dynamically consistent ozone fields as seen in a CCM which ultimately influence mean sea level pressure and tropospheric circulation (particularly during wintertime in the Northern Hemisphere, when ozone asymmetries are generally largest), without the computational burden of simulating interactive chemistry.

Plain Language Summary In this study we compare different methods of representing ozone (an atmospheric constituent important for heating Earth's stratosphere and driving circulation patterns) within a single climate model. Using an interactive chemistry-climate model (CCM) which calculates ozone mixing ratios allows two-way coupling between the modeled chemistry and dynamics resulting from longitudinal ozone variations but is computationally expensive. In comparison, prescribing ozone values as a climatology is computationally inexpensive but does not allow the two-way coupling present in the CCM. We introduce a novel method of prescribing an ozone climatology in such a way that it is able to maintain this two-way coupling, which is achieved by interactively rescaling the prescribed ozone values so that they are consistent with the modeled dynamics. We show that this method is able to faithfully reproduce key circulation patterns and surface conditions seen in the CCM, and as such we present it as a computationally inexpensive method for modeling interactions between ozone and dynamics to improve predictions of regional climate.

1. Introduction

Stratospheric ozone plays an important role in the Earth system, both chemically and radiatively. The optical properties of ozone allow it to heat surrounding air through absorption of shortwave or longwave radiation but also cool through emission of longwave radiation. As a result, the net contribution of ozone to total radiative heating depends strongly on altitude, latitude, and time, which substantially affects the climate and circulation (e.g., Fels et al., 1980; Forster & Shine, 1997; Hansen et al., 1997; Ramaswamy et al., 1996; Shine, 1986). Furthermore, high-latitude ozone changes, especially in the Southern Hemisphere (SH), have been shown in both observations and modeling studies to have far-reaching effects on stratospheric chemistry, circulation, as well as on surface climate (e.g., Braesicke et al., 2013; Iglesias-Suarez et al., 2016; Keeble et al., 2014; McLandress et al., 2011; Perlwitz et al., 2008; Polvani et al., 2011; Roscoe et al., 2003; Son et al., 2010; Thompson & Solomon, 2002). As a result, there have been significant advances in the

representation of stratospheric ozone in climate models over the last decade. For example, while half of the models used in Coupled Model Intercomparison Project Phase 3 (CMIP3) prescribed an invariant ozone concentration field, models in CMIP5 used either prescribed or interactive time-varying ozone fields (Eyring et al., 2013; Taylor et al., 2012). A range of models using both interactive and prescribed stratospheric ozone will be used for CMIP6 (Eyring et al., 2016). Zonally asymmetric ozone (ZAO) is automatically generated in state-of-the-art coupled chemistry-climate models (CCMs), which use an interactive chemistry model coupled to a global circulation model (GCM). These models can resolve a range of chemistry-climate interactions, with the distribution of stratospheric ozone consistent with the model's dynamics and other chemical fields. However, due to the high computational cost of running interactive chemistry, many models continue to prescribe stratospheric ozone as a time-varying field. This is typically done either as a zonal-mean (2-D) field or a climatological 3-D field: when prescribed as a zonally symmetric field the effects of ZAO on stratospheric circulation are not represented at all within the GCM, and prescribing a climatological 3-D ozone field results in the chemical ozone field being inconsistent with the model's dynamics for any given time step. Both configurations prevent dynamical zonal asymmetries from feeding back onto the zonal distribution of ozone (by the transport of ozone through advection), and hence also on radiative heating, as occurs in fully interactive systems. As a result, chemical-radiation-dynamical feedback processes are not addressed in GCMs with zonal-mean ozone specifications, and this may be a significant limiting factor in the model's ability to accurately represent the atmosphere and relevant processes.

In the lower stratosphere, where the chemical lifetime for ozone is long, distributions of ozone are largely controlled by transport. In the polar lower stratosphere during wintertime, zonal asymmetries in dynamics arising from waves and eddies may produce substantial zonally asymmetric features in the distribution of ozone (e.g., Hartmann, 1981). Recently, zonal asymmetries in ozone have been shown to play a substantial role in driving atmospheric circulation, independent of the zonal-mean structure of ozone in the atmosphere (e.g., Albers & Nathan, 2012; McCormack et al., 2011; Silverman et al., 2017). Additionally, a number of studies have explored the extent to which stratospheric ZAO has contributed to observed dynamical trends both in the stratosphere and at the surface, over recent decades (e.g., Crook et al., 2008; Gabriel et al., 2007; Gillett et al., 2009; Peters et al., 2015; Sassi et al., 2005; Waugh et al., 2009).

Gabriel et al. (2007) showed that prescribing the observed ZAO field from the 1990–2000 December through February decadal average (using the ERA-40 reanalysis data set) resulted in dynamical trends more representative of that decade in the Arctic stratosphere compared to a simulation with zonally symmetric ozone. In terms of ozone depletion in the Arctic, there have been contrasting results on whether severe depletion events (such as the boreal winter of 2010/2011; see Manney et al., 2011) can influence tropospheric and surface conditions. Studies which have prescribed zonally symmetric ozone depletion (e.g., Karpechko et al., 2014; Smith & Polvani, 2014) have struggled to show significant surface impacts when imposing ozone depletion of observed magnitude in the Arctic stratosphere. However, studies which use interannual variability in interactive 3-D ozone fields have seen significantly different patterns in Northern Hemisphere (NH) sea level pressure between composites of the years with lowest ozone and those with highest ozone (e.g., Calvo et al., 2015; Ivy et al., 2017). While the focus of this paper is not ozone depletion, we note that from a dynamical perspective, CCMs only differ from prescribed-ozone GCMs in that their ozone field is always three-dimensional and interacts with both dynamics and composition. The fact that CCM and prescribed-ozone studies see such contrasting tropospheric responses to similar magnitudes of ozone depletion may suggest some degree of importance for ZAO in accurately representing stratosphere-troposphere coupling in the NH.

Albers and Nathan (2012) propose two pathways by which ZAO affect stratospheric temperatures, dynamics, and zonal-mean ozone: a direct radiation/dynamic impact of ZAO on local wave properties through zonally asymmetric heating (pathway P1) and an indirect effect through residual eddy transport (e.g., $\overline{v'O_3'}$) producing zonal-mean changes in ozone (pathway P2). Changes in zonal-mean ozone can also occur through changes in chemistry. When we mention P2 below, we implicitly also include any changes in chemistry which alter zonal-mean ozone. Throughout this paper, we use these properties to identify where our prescribed ZAO has a direct influence on dynamics (e.g., through the P1 pathway associated with dynamical asymmetries) and where our prescribed ZAO is unable to represent chemistry and eddy transport of ozone (e.g., through the P2 pathway associated with sharp temporal changes in the value of $\overline{O_3}$). A schematic describing these pathways within the ZAO feedback, and how they relate to our experimental design, may be found in supporting information Figure S1.

Previous studies that have looked at the dynamical effects of ZAO in the atmosphere have compared 3-D ozone fields calculated interactively by CCMs (e.g., Gillett et al., 2009; McCormack et al., 2011; Peters et al., 2015; Sassi et al., 2005; Silverman et al., 2017; Waugh et al., 2009) or prescribed from observations or CCM climatologies within simulations using the zonally averaged ozone field (e.g., Crook et al., 2008; Gabriel et al., 2007). Whether ozone asymmetries are calculated interactively or prescribed as a climatology, both approaches require either a relatively expensive fully coupled 3-D chemistry model to generate interactive ZAO or must prescribe an ozone field which is inconsistent with the modeled dynamics. When prescribing ozone as a climatological field (particularly one which is derived from monthly mean values) the model is unable to accurately resolve the typical daily magnitudes of ozone, as well as temporal changes in ozone on shorter submonthly time scales which are normally present in a coupled CCM, and this may lead to significant differences in modeled stratospheric temperatures in the Antarctic (Neely et al., 2014).

We present a novel, computationally inexpensive method for prescribing dynamically consistent ZAO from a prescribed zonal-mean climatology. The simulations used for this study target different methods of prescribing ZAO and are described in section 2, while the parametrization for calculating dynamically consistent ZAO is described in detail in section 3. We then compare the performance of three stratospheric ozone prescriptions (zonal-mean ozone, prescribed 3-D field, and the developed calculated asymmetry scheme) to a fully coupled CCM in section 4, identifying the influences of the ZAO feedback. The results are followed by a general discussion on the importance of this feedback and the appropriate use/limitations of each specified-ozone representation.

2. Experimental Design

For this study we use four simulations, one using fully coupled chemistry and three further simulations using different methods of prescribing stratospheric ozone concentrations. All four simulations use the HadGEM3-A r2.0 model (Hewitt et al., 2011), while one simulation is also coupled with the United Kingdom Chemistry and Aerosol scheme (hereafter referred to as UKCA; Figure 1). This model configuration uses N48L60 resolution, which corresponds to a horizontal resolution of 2.5° latitude by 3.75° longitude, with 60 vertical levels following a hybrid height vertical coordinate and a model top at ~84 km. The chemistry in the UKCA configuration used for this is a combination of the tropospheric (O'Connor et al., 2014) and stratospheric (Morgenstern et al., 2009) chemical schemes, which updates relevant chemical fields every model hour. This scheme includes the chemical cycles of O_x, HO_x, NO_y, Cl_y, and Br_y and the oxidation of CO, ethane, propane and isoprene. A detailed treatment of polar processes is included, with chlorine activation through heterogeneous reactions occurring on both polar stratospheric cloud particles and sulfuric acid aerosols (Morgenstern et al., 2009). The model is run with an atmospheric time step of 20 min, and chemistry is called every hour. Advection in the model is semi-Lagrangian, after Priestley (1993). The radiation scheme, following Edwards and Slingo (1996), includes nine longwave bands and six shortwave and is updated every six model hours; ozone and its asymmetries feed back on the dynamics through their effects on radiative heating at this frequency. This model configuration has been used in the studies of Banerjee et al. (2014) and Keeble et al. (2017), in which further information can be found.

A time slice integration using the UKCA model was run under perpetual year 2000 boundary conditions for 50 years. These boundary conditions include long-lived greenhouse gas, ozone-depleting substances, aerosol loadings, sea surface temperatures, and sea ice extent. The ozone field from this integration was then averaged over the 50 years to create both the zonal-mean and 3-D ozone climatologies, which were in turn used to prescribe ozone concentrations in a set of nonchemical GCM simulations. All integrations have the same annually repeating year 2000 boundary conditions and forcings, including sea surface temperatures, sea ice extent, greenhouse gas concentrations, and aerosol loadings. Furthermore, the multidecadal zonal-mean ozone climatology is identical between the simulations, although it may differ at any given chemical time step from the fully coupled UKCA simulation. In this way, we have defined a series of simulations which differ only in the representation of stratospheric ozone. These experiments are listed below:

1. UKCA: Perpetual-year coupled CCM forced with year 2000 boundary conditions, integrated for 50 years (identical to the TS2000 integration from Banerjee et al., 2014).
2. SPEC-ZM: Specified-composition (no chemistry) configuration of 1 with climatological monthly mean zonal-mean ozone from 1.

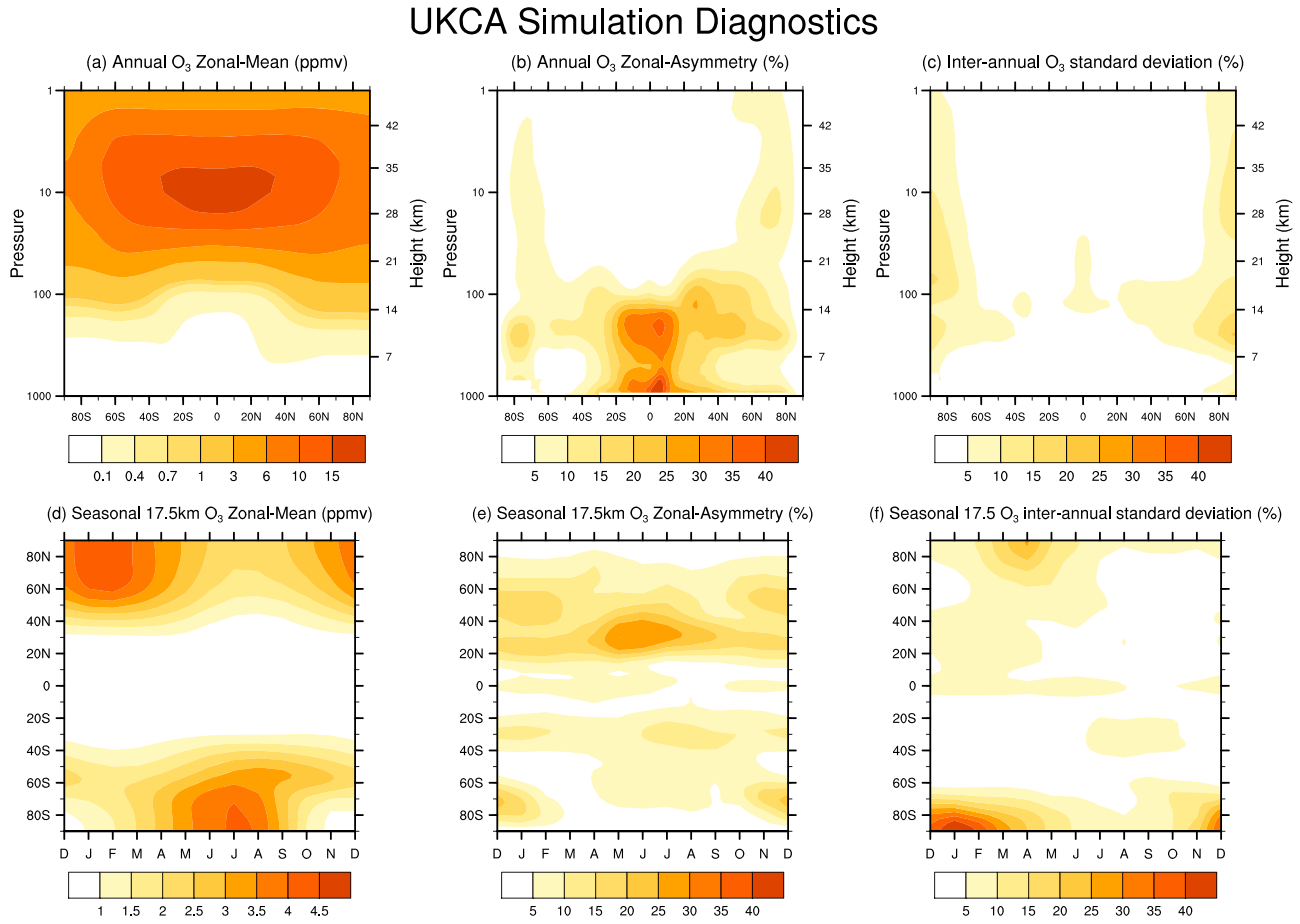

Figure 1. Annual vertical profiles (top row) and seasonal evolution at 17.5 km (bottom row) of diagnostics from the UKCA simulation. (a and d) Zonal-mean ozone $\overline{O_3}$, measured in parts per million by volume. (b and e) ZAO (monthly standard deviation of O_3'), measured as a percentage of (a) and (d), respectively. (c and f) Interannual standard deviation of monthly $\overline{O_3}$, measured as a percentage of (a) and (d), respectively. We expect that shading in (b) and (e) identifies regions where the ZAO feedback is influential in UKCA (processes which alter O_3'), and we expect that shading in (c) and (f) identifies regions where chemistry and eddy transport of ozone are most influential in UKCA (processes which alter the value of $\overline{O_3}$). UKCA = United Kingdom Chemistry and Aerosol scheme; ZAO = zonally asymmetric ozone.

3. SPEC-AZ: Specified-composition (no chemistry) configuration of 1 with climatological monthly mean 3-D ozone field from 1.
4. CALC-AZ: Specified-composition (no chemistry) configuration of 1. The zonally averaged monthly mean ozone is identical to 1 from which a dynamically consistent ZAO field is calculated online in the stratosphere (details below).

Ozone in the simulations using prescribed climatologies (experiments 2–4) is specified as a climatological field of monthly mean values, which are subsequently interpolated and updated daily. In the 3-D specification (SPEC-AZ), the tropospheric ozone values are reset to zonal mean, and prescribed asymmetries increase linearly from 0 at ~8 km and below, to full 3-D climatological values at ~11 km and above. This is to ensure all differences between specified ozone are confined to the stratosphere. Computational costs of specifying fixed ozone are the same for the zonal-mean and full 3-D climatologies (SPEC-ZM, SPEC-AZ, and CALC-AZ), which are roughly 3–4 times faster than the full CCM. We prescribe ZAO in our simulations SPEC-AZ and CALC-AZ independent of zonal-mean ozone; covariance between prescribed ZAO and meridional/vertical winds does not produce a net transport in ozone (as it would in a CCM or Earth's atmosphere) because the zonal-mean distribution is fixed from the UKCA climatology. The following section discusses the treatment of ozone in the CALC-AZ integration, where zonal asymmetries for stratospheric ozone are actively calculated.

3. Calculating a Dynamically Consistent Ozone Field while Using Prescribed Values

The purpose of CALC-AZ is to generate interactively a 3-D ozone field which follows the spatial patterns of potential vorticity (PV), but which also maintains exactly the prescribed zonal-mean climatology of both SPEC-ZM and SPEC-AZ. To do this, PV is first calculated at each radiation time step. This is then normalized, as in Allen and Nakamura (2003), so that it can function as an equivalent latitude coordinate. We define our equivalent latitude coordinate φ_q as follows:

$$\varphi_q = \operatorname{asin}\left(\frac{2q - q_{\max} - q_{\min}}{q_{\max} - q_{\min}}\right) \in \left[-\frac{\pi}{2}, \frac{\pi}{2}\right] \tag{1}$$

where q is PV and max/min refer to the global extrema of this field, on each model level. Here, this coordinate is used to generate a dynamically evolving 3-D field from a 2-D reference state (using the specified 2-D zonal-mean ozone climatology from UKCA, SPEC-ZM). If zonal-mean ozone is specified in terms of height and latitude, then the equivalent latitude specification can act as an effective extension to a 3-D field:

$$Z(\lambda, \varphi, z) = \overline{\mathrm{O_3}}\left(\varphi_q(\lambda, \varphi, z), z\right) \tag{2}$$

where λ is longitude, φ is latitude, z is model level, the overbar denotes the specified zonal-mean ozone distribution, and φ_q is the equivalent latitude coordinate. The expression on the LHS, $Z(\lambda, \varphi, z)$, is explicitly 3-D while the expression on the RHS is explicitly 2-D, but within the φ_q coordinate has implicit 3-D structure. This zonal-mean value of the 3-D field is not constrained at every time step, so it must be rescaled to match the specifying reference state in the zonal mean, thereby ensuring that the specified zonal-mean climatology is reproduced exactly in the resulting zonally asymmetric field that is seen by the radiation scheme:

$$\mathrm{O_3}(\lambda, \varphi, z) = \overline{\mathrm{O_3}}(\varphi, z) + \alpha Z'(\lambda, \varphi, z) \tag{3}$$

where $'$ indicates that the zonal mean has been removed and α is an asymmetry-scaling coefficient (could be any function of height, latitude, and/or time) by which to scale the asymmetry. In this study, the scaling factor is computed by regressing $\mathrm{O_3}'$ against Z' in UKCA, such that

$$\alpha = \frac{\overline{Z'\mathrm{O_3}'}}{\overline{Z'Z'}} \tag{4}$$

is a climatological function of month, height, and latitude. Defined this way, the scaling factor contains information of the underlying model's behavior of dynamical asymmetry and how ZAO varies with those asymmetries, which is most likely to produce an accurate realization of the UKCA stratosphere in general.

The scaling coefficient α (vertical profile shown in Figure 2a as an annual average) is designed to suppress the formation of PV-based ZAO in regions where these would not normally arise, such as the troposphere (where ZAO might be dominated, for example, by surface emissions of precursors, deposition, and stratosphere-troposphere exchange) and uppermost stratosphere (where ZAO is dominated by diurnal cycles of available shortwave radiation). In these regions, a PV-based ozone scheme is not appropriate and so our ability to accurately capture the dynamics of UKCA is limited. To adjust for this, we set $\alpha = 0$ below ~8 km, above which it increases linearly to the expression defined in equation (4) around ~11.5 km and remains as such until the model top at ~84 km.

Figure 2b shows the latitude-time climatological evolution of our regression-calculated fitting coefficient α at around 17.5 km, where, as indicated by the solid contours, the P1 and P2 pathways are expected to be important. Positive values of α identify regions where ZAO are driven by dynamical processes (related to our equivalent latitude field Z) and where we expect the P1 pathway to be most influential. The dashed contours of Figure 2 outline where ZAO is suitably large but α is negative, suggesting that the existing ZAO is not driven by dynamics and is instead related to other processes within the P2 pathway which can influence $\mathrm{O_3}'$ (such as heterogeneous chemistry). Outside of the solid contoured region, there are large fluctuations in the value of α, particularly in the tropics. However, the magnitude of ZAO in the tropics is small.

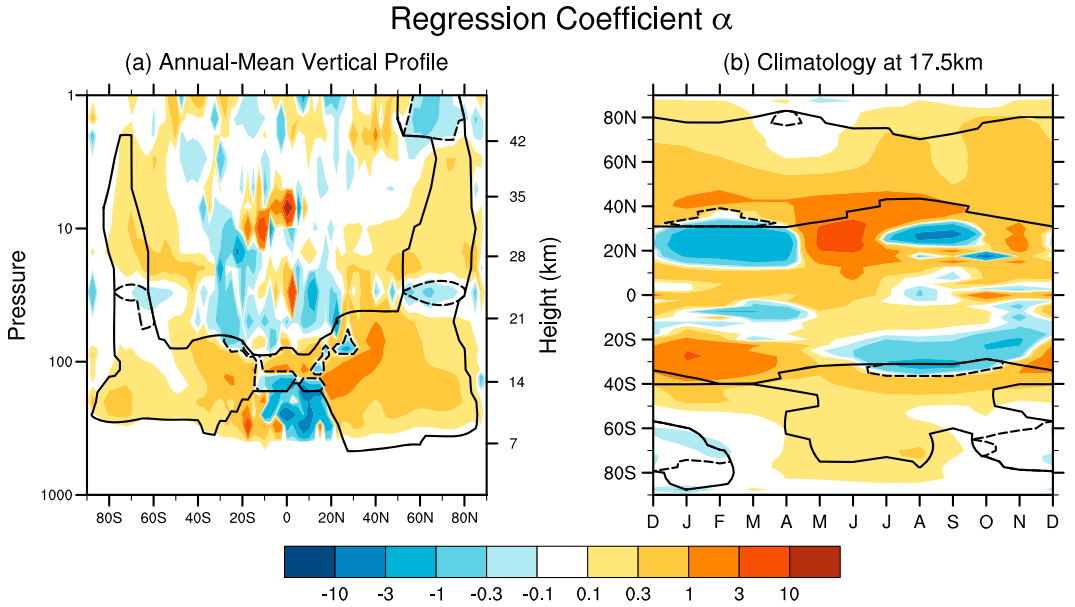

Figure 2. The scaling factor α from equation (4) shown as (a) an annual-mean vertical profile, and (b) as a climatology at the 17.5-km level. The solid contours in (a)/(b) denote regions which are shaded in Figures 1a and 1b/1d and 1e, where the magnitude of ZAO is large and provides us with an estimate of where we expect the ZAO feedback to be most active. The value of α is almost exclusively positive in the solid contoured region. However, regions where α is negative (dashed contours) are strongly associated with regions of high interannual variability in $\overline{O_3}$ in Figures 1c and 1f. This dashed contoured region indicates where ZAO is dominated by chemistry and eddy transport of ozone in UKCA, and where prescribed ZAO may not be representative of a CCM. CCM = chemistry-climate model; UKCA = United Kingdom Chemistry and Aerosol scheme; ZAO = zonally asymmetric ozone.

The following section will detail the differences from each of the prescribed ozone simulations, relative to the CCM. We will begin by discussing the relationship between PV and ozone in each simulation, followed by a detailed analysis of winter and springtime dynamics at high latitudes, focusing on the polar vortex in each hemisphere. All differences will be due to the nature of the specified ozone representation (all other boundary conditions and forcings being identical).

4. Results

To quantify the impacts on temperature and circulation of prescribing stratospheric ozone climatologies with different ZAO on temperature and circulation, we must first examine the behavior of ozone in each simulation which is ultimately driving our model differences. We can then compare the climatological performance of each of the noninteractive simulations using prescribed ozone to the fully coupled UKCA simulation. In this way we can identify which method results in the least divergence from the UKCA simulation and so could be said to have performed best.

4.1. Ozone

Examples of the different ozone representations are shown for the NH in Figure 3, where the spatial distribution of ozone (color shading) at 17.5 km and PV (black contours) at 70 hPa in March are given for two example years from each simulation. One year from each simulation shows the lowest spatial correlation between O_3 and PV poleward of 40° (top row), with the highest spatial correlation shown in the bottom row. The figure highlights the interannual variability in the very good spatial correlation between ZAO and large-scale dynamical features in the fully coupled UKCA and CALC-AZ simulations, as well as the inconsistencies introduced between dynamical features and ozone distributions when fixed ozone is prescribed in both SPEC-ZM and SPEC-AZ. It also shows that the year with the lowest spatial correlation in UKCA (top left) occurs when there is substantial ozone depletion in the Arctic lower stratosphere, which reinforces the idea that the regression coefficient α should be small (if not negative) in regions where P2 processes such as heterogenous ozone chemistry regularly occur. Since the dynamics in SPEC-AZ are close to

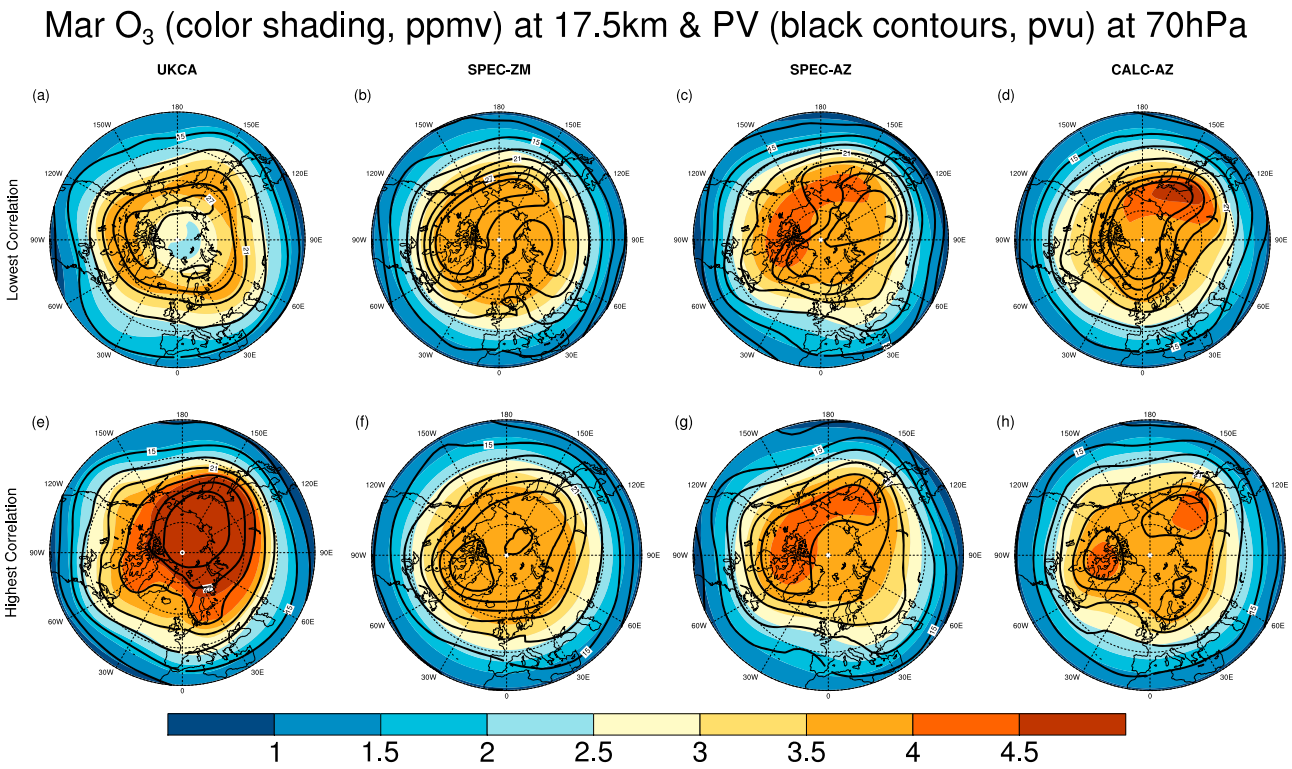

Figure 3. Arctic stereographs of stratospheric ozone at 17.5 km (color shading, ppmv) and distributions of potential vorticity at 70 hPa (black contours, pvu) during March for years with the lowest PV/O_3 spatial correlation (a–d) and for years with the highest PV/O_3 spatial correlation (e–h), shown for each of the different representations of stratospheric ozone (columns). Ozone in both UKCA (a, e) and CALC-AZ (d, h) may be altered by model dynamics at any given time step, while the distribution of ozone in SPEC-ZM (b, f) and SPEC-AZ (c, g) is the same every year for any given month. PV = potential vorticity.

that of UKCA in general, there will be instances where the instantaneous PV is aligned with the prescribed climatological 3-D ozone field (Figures 3e–3h); however, this is not always the case (Figures 3a–3d).

Analogous to Figure 3, Figure 4 depicts examples of September in the SH during the years of lowest (top row) and highest (bottom row) spatial correlation between PV and ozone. Much like the NH, the year with the lowest PV/ozone spatial correlation also has reduced polar cap ozone compared to the year of highest ozone (Figures 4a and 4e). Heterogeneous ozone losses occur on an annual basis in UKCA's Antarctic stratosphere, and this can be seen in the climatological ozone prescribed in both SPEC-ZM (Figures 4b and 4f) and SPEC-AZ (Figures 4c and 4g), as well as in CALC-AZ (Figures 4d and 4h). Since ZAO here is dominated by heterogeneous chemistry, the value of α in the SH during September is small (Figure 2b), and so CALC-AZ consistently underestimates the total magnitude of ZAO in the Antarctic.

Both Figures 3 and 4 show that ozone (color shading) generally adapts to the dynamical PV patterns (black contours) in UKCA and CALC-AZ (leftmost and rightmost panels respectively), while the monthly averaged ozone in SPEC-ZM and SPEC-AZ is the same every year (compare color shading in top and bottom rows). An important observation is that the zonal-asymmetry of CALC-AZ decreases toward the equator (more annual color shading toward the outside edges of rightmost panels), demonstrating how the magnitude of ZAO is small despite the large fluctuations of α toward the equator seen in Figures 2a and 2b (i.e., the sensitivity of ZAO to the value of α diminishes toward the equator).

4.2. Temperature and Dynamics

Our analysis of temperature and dynamics is largely confined to the lower stratosphere at high latitudes throughout the duration of the polar vortex, where the interaction between our prescription of ZAO with dynamics has a significant impact on the modeled stratosphere. Significant temperature differences arising outside of the polar vortex are not related to our prescription of ZAO and are not considered in this section Additional information on differences during the final warming may be found in Figures S2 and S3 of the supporting information for the Northern and Southern Hemispheres, respectively. The following sections

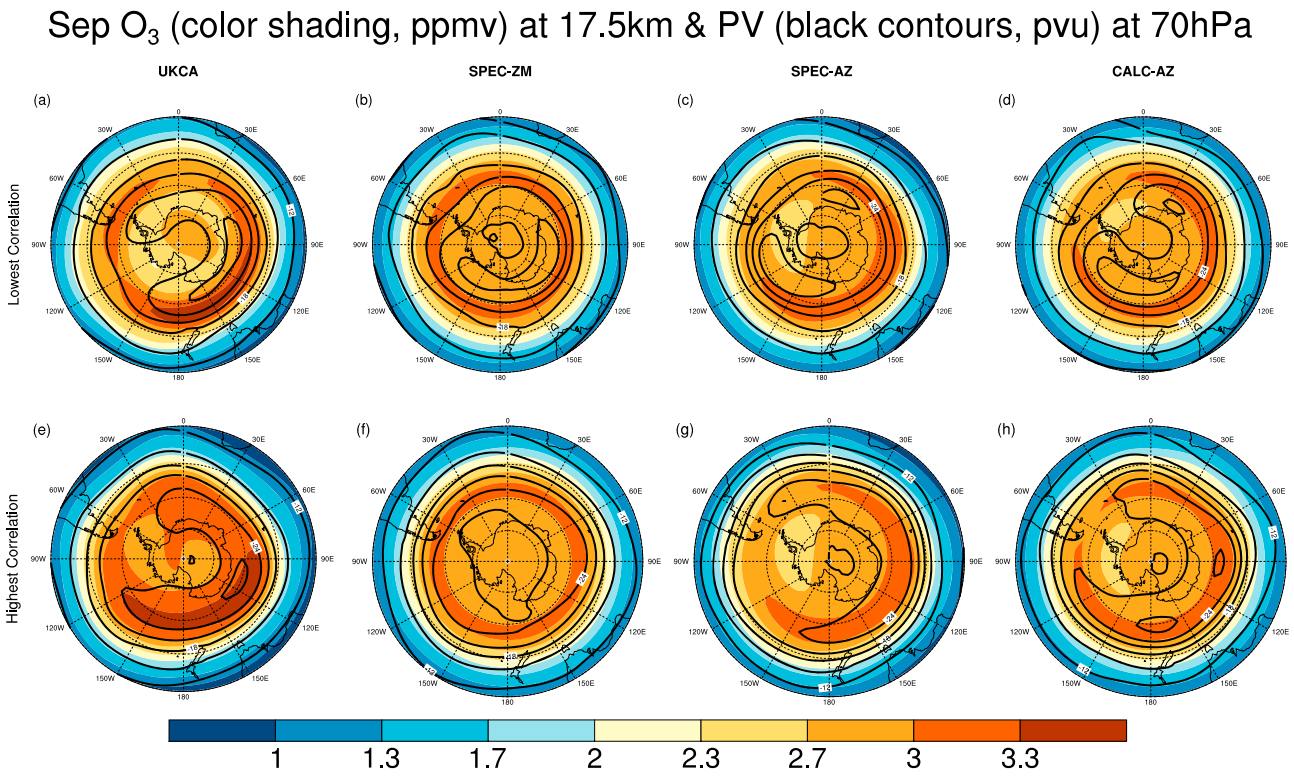

Figure 4. Same as Figure 3 but showing Antarctic stereographs during September during the years of lowest (a–d) and highest (e–h) spatial correlation between potential vorticity and ozone. The dynamical behavior in the Southern Hemisphere is more similar across simulations than the Northern Hemisphere in Figure 3. This is because the dynamical asymmetry of the Antarctic stratosphere is generally smaller than that of the Arctic, but it may also be influenced by our choice of the UKCA model for our interactive simulation, which has been shown to underrepresent the degree of zonal asymmetry seen in observational analyses (Dennison et al., 2017). PV = potential vorticity.

examine 50-year climatological differences from each hemisphere in detail. Color shading in figures presented throughout this section only shows features which are statistically significant at the 95% confidence interval, as measured by a two-tailed *t* test. Regions where changes are not significant to this confidence interval have been masked out and are deemed suitably similar to UKCA to be excused from our analysis.

4.2.1. NH Differences

Figure 5 shows the zonal-mean temperature differences in the NH during both the wintertime (December through March, DJFM), when the magnitude of ZAO is large (Figure 1e), and the springtime (April through June) when the Arctic vortex breaks up and easterlies descend into the lower stratosphere. The figure highlights the zonal-mean temperature differences from UKCA in the Arctic stratosphere during two periods of interest: the wintertime vortex (top row) and the final warming (bottom row).

Figures 5a–5c show that the Arctic vortex is too cold relative to UKCA when zonally symmetric ozone is prescribed in SPEC-ZM (Figure 5a). We attribute this polar cap temperature difference to a suppression in vertical wave flux entering the Arctic stratosphere in SPEC-ZM, reducing poleward eddy heat transport and the dynamical heating of the vortex in this simulation. Figures 5b and 5c show that these differences in the lower stratosphere are remedied to within 0.25 K of UKCA when ZAO is included in either SPEC-AZ or CALC-AZ. Vector differences are consistently more upward pointing in SPEC-AZ and CALC-AZ compared to SPEC-ZM within the solid contoured region during DJFM, which demonstrates the physical role of ZAO in enhancing planetary wave activity in the Arctic vortex during wintertime.

Figures 5d–5f show that zonal-mean temperature differences in the Arctic stratosphere are within 1 K of UKCA in all simulations during and shortly after the time of final warming, which occurs on average around mid-April in all of our simulations. During this time of year, easterly winds descending into the lower stratosphere significantly reduce planetary wave activity, and the influence of ZAO on stratospheric dynamics

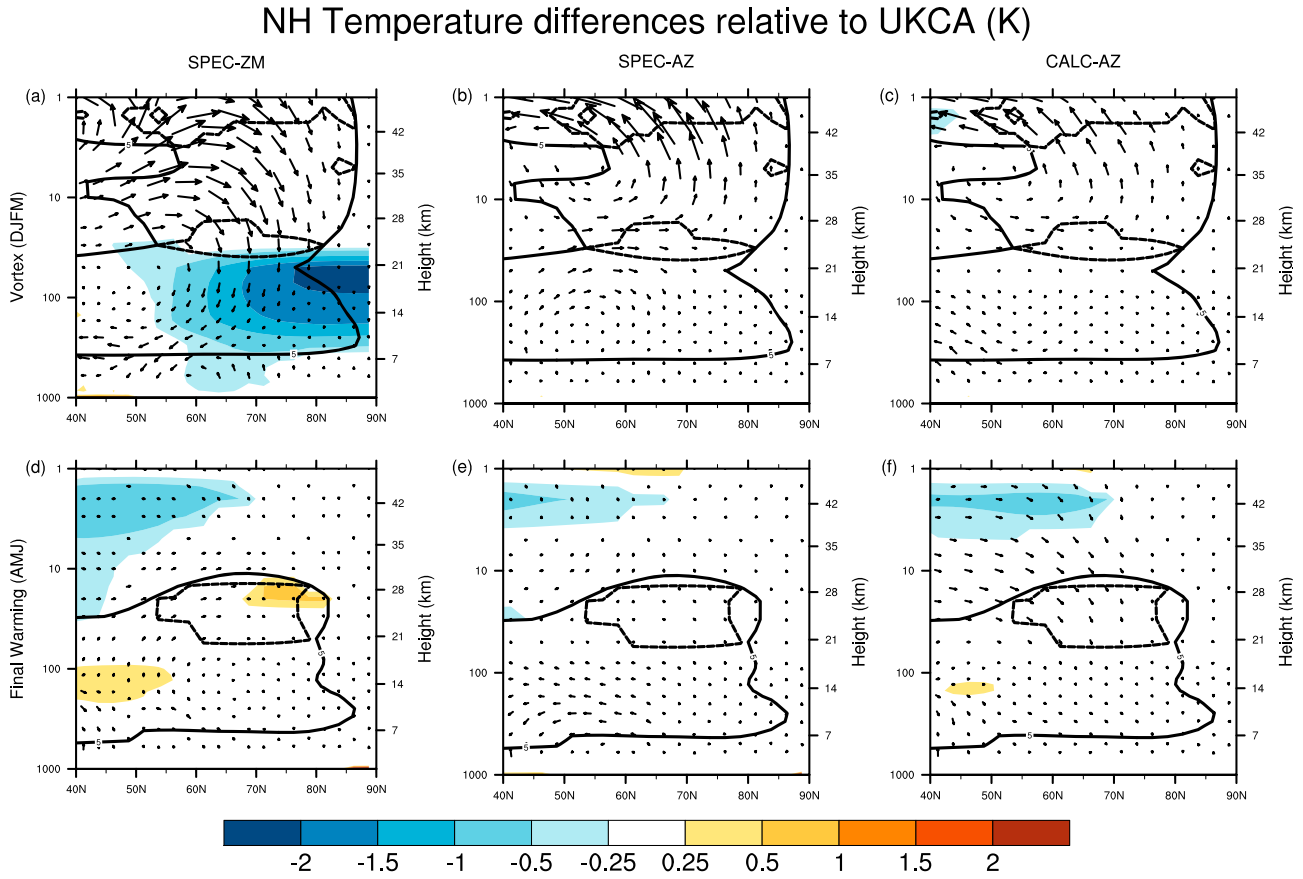

Figure 5. Vertical profiles of zonal-mean temperature differences for each of the prescribed-ozone simulations relative to UKCA: SPEC-ZM (a, d), SPEC-AZ (b, e), and CALC-AZ (c, f). The top row shows these differences during December through March (to show the wintertime polar vortex) and the bottom row during April through June (to show the final warming). Color shading is only present when changes are statistically significant at the 95% confidence interval. Overlaid are Eliassen-Palm flux vector differences, scaled by $1/\rho_0$, with the vertical component scaled by an additional $5\pi r_e/756$ km to more accurately depict the orientation of the vectors in the frame. The solid and dashed contours are analogous to those in Figure 2. NH = Northern Hemisphere.

becomes severely limited. As a result, the zonal-mean temperature differences in SPEC-ZM, SPEC-AZ, and CALC-AZ look very similar during April through June (Figures 5d–5f).

The results presented above indicate that SPEC-AZ and CALC-AZ both result in modeled wintertime Arctic stratospheric zonal-mean temperatures which are consistent with UKCA. In contrast, Figure 6 shows Arctic stereographs of differences in PV (top row), temperature (middle row), and mean sea level pressure (MSLP; (bottom row) during NJFM between each simulation (columns) and UKCA.

An interesting feature is the pattern of PV differences which arise in the SPEC-ZM and SPEC-AZ simulations. The significant enhancement of Arctic PV in SPEC-ZM at 450 K (Figure 6a) is very annular in shape, and closer inspection reveals that PV is further enhanced over northern Canada, where ozone in UKCA is higher on average (as seen in the prescribed SPEC-AZ ozone field in Figures 3c and 3g). In SPEC-AZ, the fixed ZAO pattern of lower ozone over the northern Eurasian continent (see Figures 3c and 3g) results in a climatological shift in the Arctic vortex toward Scandinavia and Siberia (Figure 6b). In contrast, the dynamically generated ZAO in CALC-AZ produces no climatological shift in the Arctic vortex and PV differences at 450 K compared to UKCA are very small (Figure 6c).

The temperature differences at 70 hPa in Figures 6d–6f show similar patterns to the PV differences, particularly the symmetric differences in SPEC-ZM (Figure 6d) and the lack of significant differences in CALC-AZ (Figure 6f). The zonal-mean DJFM temperature differences in SPEC-AZ from Figure 5 showed no significant patterns in much of the NH; however, Figure 6b shows that the North Atlantic region is too cold compared to UKCA. Finally, Figure 6g–6i show the climatological differences in MSLP and highlights a significant

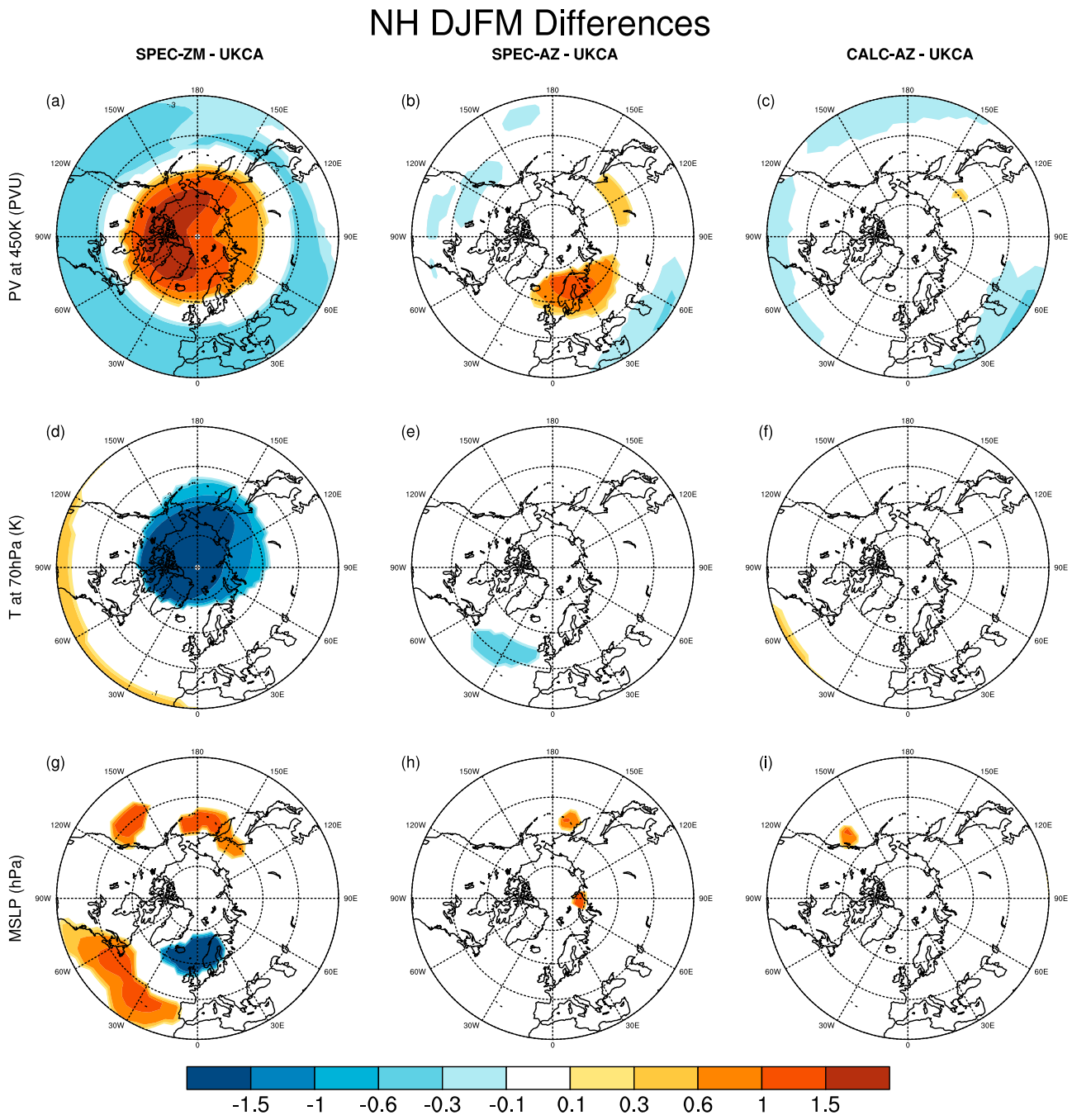

Figure 6. Arctic stereographs of (a–c) PV differences at 450 K (pvu), (d–f) temperature differences at 70 hPa (K), and (g–i) MSLP (hPa). Color shading is only present where differences from UKCA are statistically significant at the 95% confidence level. The pattern of significant PV differences in SPEC-ZM and SPEC-AZ reflect the symmetry of the prescribed ozone in these simulations (which can be seen in the color shading of Figure 3). DJFM = December through March; MSLP = mean sea level pressure; NH = Northern Hemisphere; PV = potential vorticity.

change in the modeled North Atlantic Oscillation (NAO) in SPEC-ZM, which has implications for North Atlantic storm tracks and surface conditions across Europe. Using zonal-mean ozone forcing results in unrealistic surface pressure patterns when compared to UKCA (or with SPEC-AZ or CALC-AZ).

4.2.2. SH Differences

We now consider differences in the SH during both the wintertime (July through October), when the magnitude of ZAO is large (though not as large as in the NH winter, Figure 1e), and the springtime (November through January, NDJ) covering the breakup of the Antarctic polar vortex and onset of stratospheric

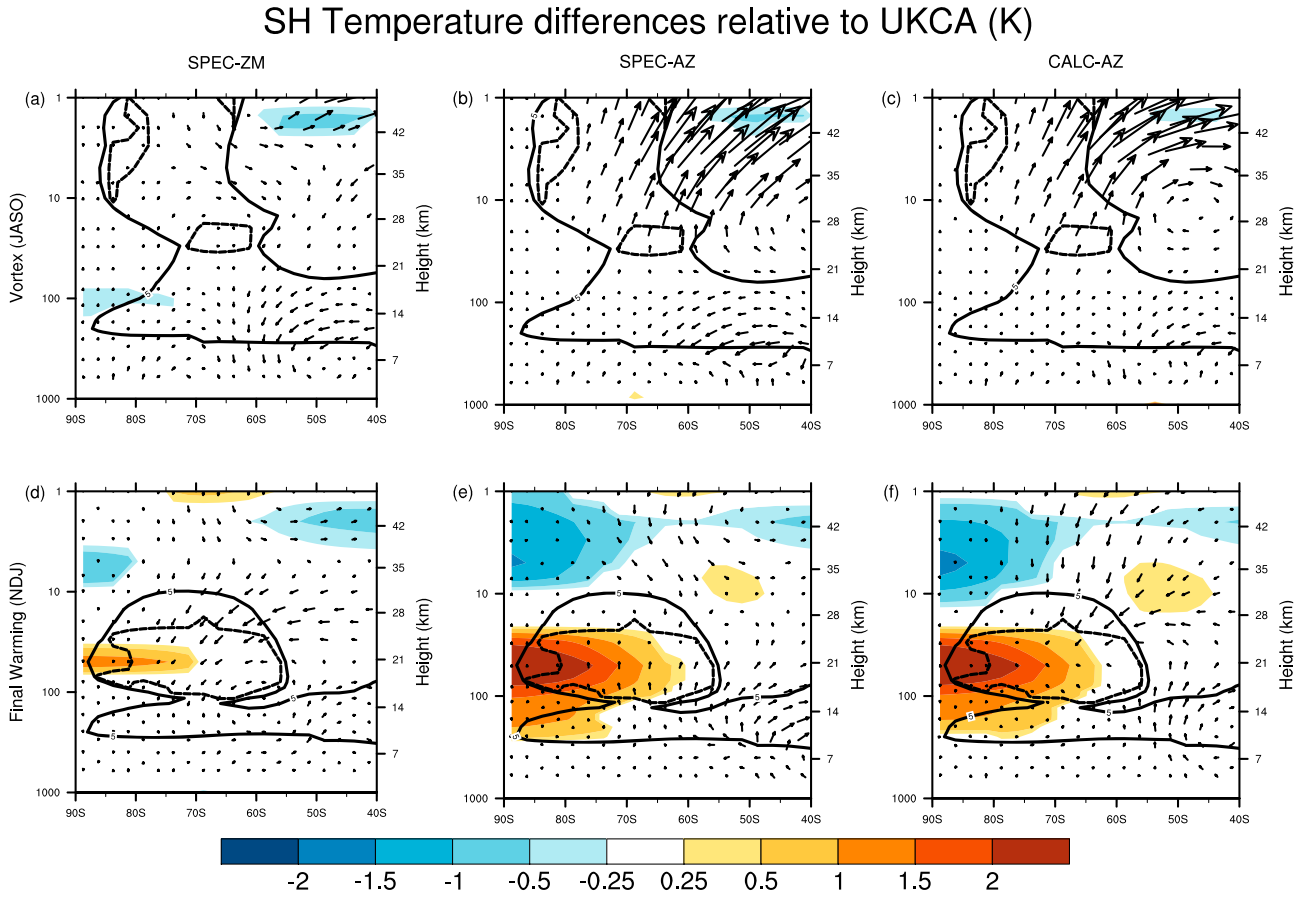

Figure 7. Same as Figure 5 but showing the Antarctic stratosphere. The differences (a–c) during JASO (to show the wintertime polar vortex) and (d–f) during NDJ (to show the final warming). JASO = July through October; NDJ = November through January.

summer. Analogous to Figure 5, Figure 7 shows the zonal-mean temperature differences in the Antarctic stratosphere during these two periods of interest, with the top row showing how the wintertime vortex differs from UKCA and the bottom row showing how the final warming differs from UKCA.

Figures 7a–7c show that zonal-mean temperatures of the wintertime Antarctic vortex are well represented by all prescribed-ozone simulations and these are within 0.5 K of the UKCA value throughout the stratosphere poleward of 60°S. Both dynamical asymmetries and ZAO are much smaller during wintertime in the Antarctic than in the Arctic (Figure 1e), and so the overall differences in ozone between the simulations are much smaller in this region. The inclusion of ZAO in SPEC-AZ (Figure 7b) and CALC-AZ (Figure 7c) leads to an increase in vertical wave flux in the solid contoured region, which was also seen in the Arctic wintertime (Figures 5b and 5c).

While the final warming was well represented in the NH (Figures 5d–5f), Figures 7d–7f show that all the prescribed-ozone simulations are unable to accurately represent the final warming SH, particularly SPEC-AZ (Figure 7e) and CALC-AZ (Figure 7f). Neely et al. (2014) showed that prescribing monthly mean climatological ozone leads to systematic biases in the temperature of the Antarctic lower stratosphere, and this undoubtedly is influencing SPEC-ZM, SPEC-AZ, and CALC-AZ equally (hence the warming in SPEC-ZM, Figure 7d). The inclusion of ZAO in SPEC-AZ and CALC-AZ is also enhancing the vertical wave flux into the lower stratosphere, which is facilitated by weakened westerlies during this period (as the descending easterlies of the final warming do not reach down to this level in the SH). The enhancement of vertical wave flux further warms and weakens the Antarctic vortex in SPEC-AZ (Figure 7e) and CALC-AZ (Figure 7f), which forces the final warming date to occur about a week earlier in these simulations (compared to 3 days earlier in SPEC-ZM). Sheshadri and Plumb (2016) suggest that differences in planetary wave activity, rather than changes in the final warming date itself, are responsible for influencing surface weather patterns around this time of year. Our results reinforce that idea, as we find the distribution of MSLP during NDJ

is most similar to UKCA in the CALC-AZ simulation with more realistic stratospheric dynamics, despite the change in final warming date. It follows that these zonal-mean temperature differences in the lower stratosphere during NDJ are caused by a small number of days with large temperature differences, rather than as a seasonally warmer Antarctic cap over the 3-month period.

According to this logic, however, the ZAO present in UKCA must also warm the Antarctic vortex in a similar manner to SPEC-AZ and CALC-AZ. We conclude that there must exist processes which are resolved only in UKCA that work to cool the vortex to counter the dynamical heating from ZAO in the simulation. Indeed, the biases described by Neely et al. (2014) are driven by processes like heterogeneous chemistry which allows zonal-mean ozone to change on time scales much shorter than a prescribed monthly mean climatology can represent. These processes in UKCA are connected to negative values of α (e.g., Figure 2) where dynamical asymmetries do not represent the behavior of ZAO in the atmosphere. Hence, the regions enclosed by the dashed contours in Figures 7d–7f highlight where heterogeneous ozone losses occur in UKCA, which keeps the vortex cold against the dynamical heating from ZAO. Furthermore, the NDJ temperature differences in the lower stratosphere are shifted slightly from the dashed contour region, highlighting the missing process of eddy transport which displaces the effects of heterogeneous chemistry from the vortex edge toward the pole in the UKCA simulation.

Since both ZAO and dynamical asymmetries are much smaller in the SH than in the NH, zonal-mean differences are more representative of the 3-D system. Nevertheless, we present a series of Antarctic stereographs in Figure 8 of PV differences at 450 K (top row, measured in potential vorticity units), temperature differences at 70 hPa (middle row, measured in kelvins), and MSLP differences (bottom row, measured in hectopascals) for each simulation (columns). The PV differences in Figures 8a–8c are all centered on the Antarctic cap and show that the Antarctic vortex is consistently too strong when ozone is prescribed compared to UKCA. In SPEC-AZ, these PV differences are significant more in the Western Hemisphere (and not as much in the Eastern Hemisphere), which is where the prescribed ZAO is lowest (Figures 4c and 4g). The magnitude of Antarctic ZAO is underestimated during wintertime in all prescribed-ozone simulations compared to UKCA because we are unable represent ZAO arising from heterogeneous chemistry, and this decreased ZAO leads to a stronger and more circular vortex in these simulations.

The temperature differences from UKCA at 70 hPa are largely insignificant in all simulations, although the Antarctic vortex in SPEC-ZM shows some significant differences well within 1 K over the continent (Figure 8d). All simulations overestimate MSLP in the Weddell sea (Figures 8g–8i), although both SPEC-ZM (Figure 8g) and SPEC-AZ (Figure 8h) show small but significant MSLP differences in other parts of the SH.

4.3. Other Features

There are some consistent differences between UKCA and each of the three prescribed-ozone simulations, which result from factors other than the direct interaction of ZAO and dynamics through the P1 pathway. For example, all prescribed ozone simulations show a large temperature increase in the uppermost stratosphere and mesosphere, of about 17 K above 1 hPa, below which there is significant cooling of about 0.5 K between 60°S and 60°N extending into the tropical midstratosphere (not shown). This feature in the mesosphere was described by Sassi et al. (2005), and these high-altitude temperature differences have also been remarked upon in studies by Gillett et al. (2009), McCormack et al. (2011), Peters et al. (2015), and Silverman et al. (2017) all of which compare zonally averaged ozone in a CCM to a fully interactive configuration. Sassi et al. (2005) attribute this feature to the nonlinear addition of variations in radiative heating over diurnal cycles and bands of longitude, that acts only on the diurnal component of ZAO (this dominates the ZAO pattern in the mesosphere and tropical upper stratosphere).

Finally, we see a robust shift in the frequency (speeding up) of the quasi-biennial oscillation (QBO) in our experiments which prescribe the zonal-mean value of ozone. The Unified Model has an internally generated QBO, which in the interactive UKCA simulation used for this study has a period of approximately 32 months. When ozone fields are prescribed, the QBO period becomes shorter; ~29 months in SPEC-ZM and in CALC-AZ, and ~30 months in SPEC-AZ. All three of these simulations show significant cooling in the tropical upper stratosphere extending into midlatitudes, mentioned above. The small temperature decreases in this region suggest a general strengthening of tropical upwelling (vertical velocities from these simulations were not available, unfortunately), which would provide a consistent link with the shortening of the QBO period (e.g., Kawatani & Hamilton, 2013) in these simulations which prescribe ozone compared to UKCA. A recent

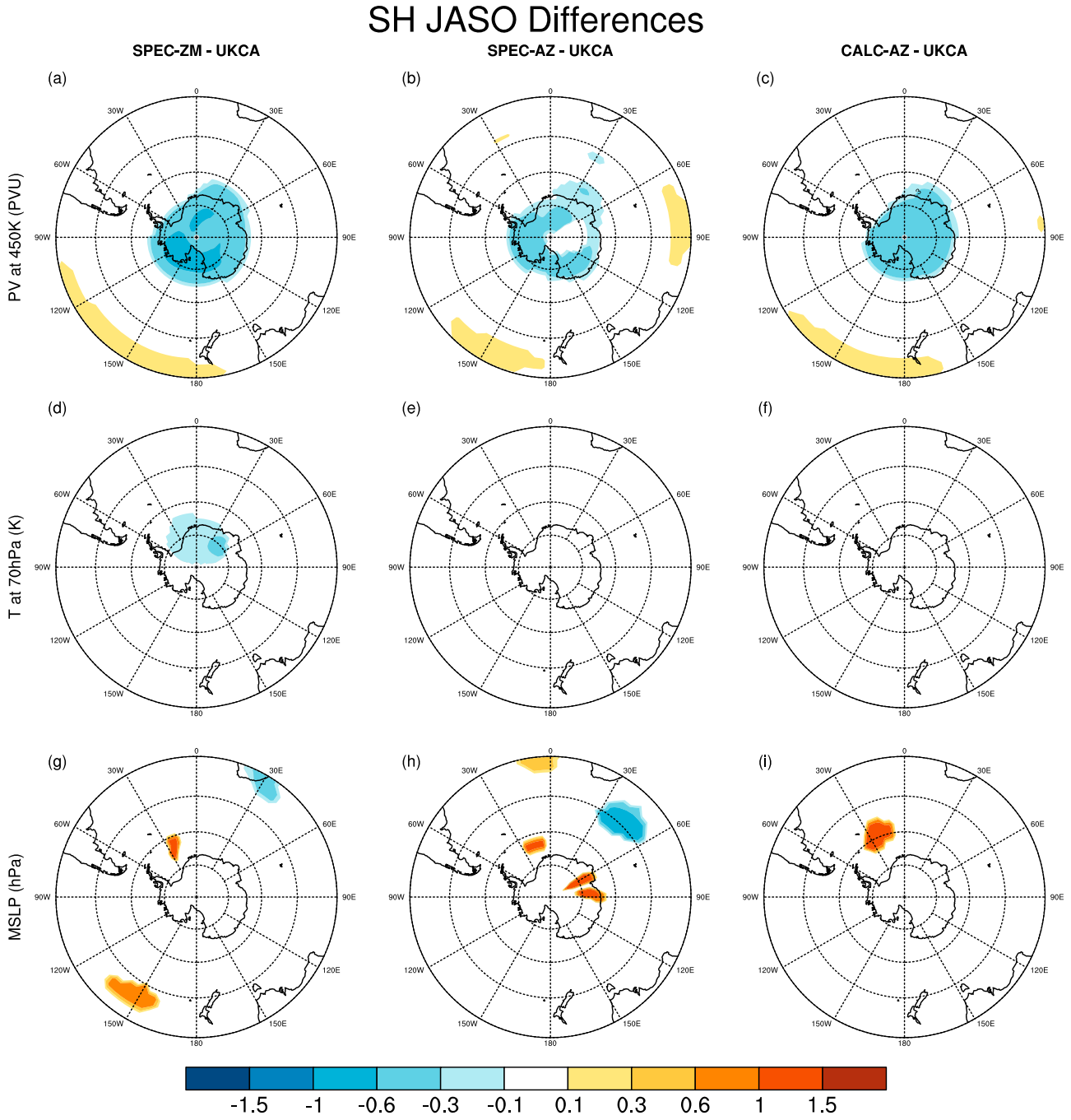

Figure 8. Same as Figure 6 but showing the Antarctic stereographs during JASO. JASO = July through October; MSLP = mean sea level pressure; PV = potential vorticity; SH = Southern Hemisphere.

study by Silverman et al. (2017) has provided evidence that the QBO may modulate ZAO at midlatitudes. However, our results indicate that ZAO can in turn influence the QBO, a conclusion which can only be reached by using a model with an internally generated QBO (such as UKCA), setting up the possibility for two-way interactions between ZAO and the QBO.

5. Conclusions

In both Earth's atmosphere and in a CCM, dynamical asymmetries in the polar lower stratosphere produce ZAO, which in turn feeds back onto stratospheric dynamics through both radiative heating (P1 pathway)

and through eddy transport (P2 pathway). We have introduced a novel method of generating ZAO interactively within a GCM from a prescribed zonal-mean ozone climatology, providing a complete representation of the P1 pathway without the computational burden of using ozone from a CCM. When ozone is generated in this manner (our CALC-AZ simulation) the high-latitude dynamics in the modeled lower stratosphere closely resemble those of UKCA and do not exhibit most of the strong biases associated with prescribing either zonally symmetric ozone (SPEC-ZM) or fixed climatological asymmetries (SPEC-AZ) in these parts of the atmosphere.

In the Arctic stratosphere, the exclusion of ZAO in the SPEC-ZM simulation results in a colder, more polar-centric vortex compared to a CCM; this has a significant impact on the wintertime NAO and therefore affects tropospheric circulation. The inclusion of ZAO increases planetary wave flux into the lower stratosphere, heating the Arctic vortex and reducing the differences in both vortex strength and MSLP. However, prescribing fixed climatological ZAO in SPEC-AZ shifts the polar vortex toward Scandinavia in the climatological average, where ozone in the prescribed field takes its lowest value. It is only when dynamically consistent ZAO are included in the CALC-AZ simulation, thereby completing the P1 pathway, that the Arctic vortex is consistent with that modeled in the interactive UKCA simulation in both strength and position, and the MSLP differences are minimized.

In the Antarctic stratosphere, dynamical asymmetries play a more limited role in generating ZAO, which are largely driven by heterogeneous chemistry in and around the polar vortex. Overall, the net differences between SPEC-ZM and UKCA are smaller compared to the Arctic, but are similar in that the vortex is colder and more circular during wintertime. Much like the Arctic but to a lesser degree, SPEC-AZ shows a climatological shift toward west Antarctica where the climatological ozone field is lowest. Nevertheless, the Antarctic vortex is too circular in all simulations compared to UKCA because they all neglect ZAO from heterogeneous chemistry. It is only around the time of final warming that differences from prescribed ZAO start to emerge, in that both SPEC-AZ and CALC-AZ force the final warming date to occur about a week earlier than in UKCA (and half a week earlier in SPEC-ZM). These differences in final warming date are related to the lack of temporal resolution in our ozone specification and its inability to resolve heterogeneous chemistry (and other P2 processes), rather than from dynamical differences (the effects of which cancel each other out quite well in SPEC-ZM's Antarctic vortex). Despite this earlier final warming, the dynamical ZAO is well represented by CALC-AZ and shows the smallest differences from UKCA in both vortex shape and in MSLP throughout the season, much like in the Arctic.

One of the most practical uses for GCMs is to predict systematic changes in regional surface conditions, such as temperatures and weather patterns, into the future. If certain regional biases in MSLP can be removed by generating ZAO from a model's internal dynamics, which we have proven possible, then this approach should be prioritized for improving the accuracy of any climate simulation which does not require chemical predictability (or for which future composition is specified). The methodology presented here is a computationally inexpensive way of achieving this and is suitable for further modeling studies. Looking forward we may be able to generate ZAO in this way from a simplified 2-D chemistry model, rather than a prescribed climatology, which would add chemical predictability as well as a complete representation of the P2 pathway (eliminating the remaining biases to do with heterogeneous chemistry and eddy transport) without the expensive computation of coupling full 3-D chemistry.

Acknowledgments
This work was made possible by the U.K. Natural Environment Research Council. The research leading to these results has received funding from the European Community's Seventh Framework Programme (FP7/2007–2013) under grant agreement 603557 (StratoClim) and the European Research Council through the ACCI project (project 267760). We thank NCAS-CMS for modeling ort. Model integrations have been performed using the ARCHER UK National Supercomputing Service (http://www.archer.ac.uk). The code changes used to produce this data may be found in the svn://puma/UM_svn/UM repository, under the branch fcm:um_br/dev/s1016670/vn7.3_DynamicOzone73/src under revision number 22598, while the data used for this work may be found on the JASMIN data analysis system within the UKCA group workspace.

References

Albers, J. R., & Nathan, T. R. (2012). Pathways for communicating the effects of stratospheric ozone to the polar vortex: Role of zonally-asymmetric ozone. *Journal of the Atmospheric Sciences*, *69*, 785–801. https://doi.org/10.1175/JAS-D-11-0126.1

Allen, D. R., & Nakamura, N. (2003). Tracer equivalent latitude: A diagnostic tool for isentropic transport studies. *Journal of the Atmospheric Sciences*, *60*, 287–304. https://doi.org/10.1175/1520-0469(2003)060<0287:TELADT>2.0.CO;2

Banerjee, A., Archibald, A. T., Maycock, A. C., Telford, P., Abraham, N., Yang, X., et al. (2014). Lightning NO_x, a key chemistry–climate interaction: Impacts of future climate change and consequences for tropospheric oxidising capacity. *Atmospheric Chemistry and Physics*, *14*(18), 9871–9881. https://doi.org/10.5194/acp-14-9871-2014

Braesicke, P., Keeble, J., Yang, X., Stiller, G., Kellmann, S., Abraham, N. L., et al. (2013). Circulation anomalies in the Southern Hemisphere and ozone changes. *Atmospheric Chemistry and Physics*, *13*(21), 10677–10688. https://doi.org/10.5194/acp-13-10677-2013

Calvo, N., Polvani, L. M., & Solomon, S. (2015). On the surface impact of Arctic stratospheric ozone extremes. *Environmental Research Letters*, *10*, 094003. http://doi.org/10.1088/1748-9326/10/9/094003

Crook, J. A., Gillett, N. P., & Keeley, S. P. (2008). Sensitivity of Southern Hemisphere climate to zonal asymmetry in ozone. *Geophysical Research Letters*, *35*, L07806. https://doi.org/10.1029/2007GL032698

Dennison, F., McDonald, A., & Morgenstern, O. (2017). The evolution of zonally asymmetric austral ozone in a chemistry-climate model. *Atmospheric Chemistry and Physics*, *171*, 14,075–14,084. http://doi.org/10.5194/acp-17-14075-2017

Edwards, J., & Slingo, A. (1996). Studies with a flexible new radiation code. I: Choosing a configuration for a large-scale model. *Quarterly Journal of the Royal Meteorological Society*, *122*, 689–719. https://doi.org/10.1002/qj.49712253107

Eyring, V., Arblaster, J., Cionni, I., Sedláček, J., Perlwitz, J., Young, P. J., et al. (2013). Long-term ozone changes and associated climate impacts in CMIP5 simulations. *Journal of Geophysical Research: Atmospheres*, *118*, 5029–5060. https://doi.org/10.1002/jgrd.50316

Eyring, V., Bony, S., Meehl, G. A., Senior, C. A., Stevens, B., Stouffer, R. J., & Taylor, K. E. (2016). Overview of the Coupled Model Intercomparison Project Phase 6 (CMIP6) experimental design and organization. *Geoscientific Model Development*, *9*(5), 1937–1958. https://doi.org/10.5194/gmd-9-1937-2016

Fels, S. B., Mahlman, J. D., Schwarzkopf, M. D., & Sinclair, R. W. (1980). Stratospheric sensitivity to perturbations in ozone and carbon dioxide: Radiative and dynamical response. *Journal of the Atmospheric Sciences*, *37*, 2265–2297. https://doi.org/10.1175/1520-0469(1980)037<2265:SSTPIO>2.0.CO;2

Forster, P. M. F., & Shine, K. P. (1997). Radiative forcing and temperature trends from stratospheric ozone changes. *Journal of Geophysical Research*, *102*(D9), 10,841–10,855. https://doi.org/10.1029/96JD03510

Gabriel, A., Peters, D., Kirchner, I., & Graf, H.-F. (2007). Effect of zonally asymmetric ozone on stratospheric temperature and planetary wave propagation. *Geophysical Research Letters*, *34*, L06807. https://doi.org/10.1029/2006GL028998

Gillett, N., Scinocca, J., Plummer, D., & Reader, M. (2009). Sensitivity of climate to dynamically-consistent zonal asymmetries in ozone. *Geophysical Research Letters*, *36*, L10809. https://doi.org/10.1029/2009GL037246

Hansen, J., Sato, M., & Ruedy, R. (1997). Radiative forcing and climate response. *Journal of Geophysical Research*, *102*(D6), 6831–6864. https://doi.org/10.1029/96JD03436

Hartmann, D. L. (1981). Some aspects of the coupling between radiation, chemistry, and dynamics in the stratosphere. *Journal of Geophysical Research*, *86*(C10), 9631–9640. https://doi.org/10.1029/JC086iC10p09631

Hewitt, H. T., Copsey, D., Culverwell, I. D., Harris, C. M., Hill, R. S. R., Keen, A. B., et al. (2011). Design and implementation of the infrastructure of HadGEM3: The next-generation Met Office climate modelling system. *Geoscientific Model Development*, *4*(2), 223–253. https://doi.org/10.5194/gmd-4-223-2011

Iglesias-Suarez, F., Young, P. J., & Wild, O. (2016). Stratospheric ozone change and related climate impacts over 1850–2100 as modelled by the ACCMIP ensemble. *Atmospheric Chemistry and Physics*, *16*(1), 343–363. https://doi.org/10.5194/acp-16-343-2016

Ivy, D. J., Solomon, S., Calvo, N., & Thompson, D. W. (2017). Observed connections of Arctic stratospheric ozone extremes to Northern Hemisphere surface climate. *Environmental Research Letters*, *12*, 024004. http://doi.org/10.1088/1748-9326/aa57a4

Karpechko, A. Y., Perlwitz, J., & Manzini, E. (2014). A model study of tropospheric impacts of the Arctic ozone depletion 2011. *Journal of Geophysical Research: Atmospheres*, *119*, 7999–8014. https://doi.org/10.1002/2013JD021350

Kawatani, Y., & Hamilton, K.(2013). Weakened stratospheric quasibiennial oscillation driven by increased tropical mean upwelling. *Nature*, *497*(7450), 478–481. https://doi.org/10.1038/nature12140

Keeble, J., Bednarz, E. M., Banerjee, A., Abraham, N. L., Harris, N. R., Maycock, A. C., & Pyle, J. A. (2017). Diagnosing the radiative and chemical contributions to future changes in tropical column ozone with the UM-UKCA chemistry–climate model. *Atmospheric Chemistry and Physics*, *17*(22), 13,801–13,818. https://doi.org/10.5194/acp-17-13801-2017

Keeble, J., Braesicke, P., Abraham, N. L., Roscoe, H. K., & Pyle, J. A. (2014). The impact of polar stratospheric ozone loss on Southern Hemisphere stratospheric circulation and climate. *Atmospheric Chemistry and Physics*, *14*(24), 13,705–13,717. https://doi.org/10.5194/acp-14-13705-2014

Manney, G. L., Santee, M. L., Rex, M., Livesey, N. J., Pitts, M. C., Veefkind, P., et al. (2011). Unprecedented Arctic ozone loss in 2011. *Nature*, *478*(7370), 469–475. https://doi.org/10.1038/nature10556

McCormack, J. P., Nathan, T. R., & Cordero, E. C. (2011). The effect of zonally asymmetric ozone heating on the Northern Hemisphere winter polar stratosphere. *Geophysical Research Letters*, *38*, L03802. https://doi.org/10.1029/2010GL045937

McLandress, C., Shepherd, T. G., Scinocca, J. F., Plummer, D. A., Sigmond, M., Jonsson, A. I., & Reader, M. C. (2011). Separating the dynamical effects of climate change and ozone depletion. Part II: Southern Hemisphere troposphere. *Journal of Climate*, *24*(6), 1850–1868. https://doi.org/10.1175/2010JCLI3958.1

Morgenstern, O., Braesicke, P., O'Connor, F., Bushell, A., Johnson, C., Osprey, S., & Pyle, J. (2009). Evaluation of the new UKCA climate-composition model—Part 1: The stratosphere. *Geoscientific Model Development*, *2*, 43–57. https://doi.org/10.5194/gmd-2-43-2009

Neely, R. R. III, Marsh, D. R., Smith, K. L., Davis, S. M., & Polvani, L. M. (2014). Biases in Southern Hemisphere climate trends induced by coarsely specifying the temporal resolution of stratospheric ozone. *Geophysical Research Letters*, *41*, 8602–8610. http://doi.org/10.1002/2014GL061627

O'Connor, F. M., Johnson, C. E., Morgenstern, O., Abraham, N. L., Braesicke, P., Dalvi, M., et al. (2014). Evaluation of the new UKCA climate-composition model – Part 2: The Troposphere. *Geoscientific Model Development*, *7*(1), 41–91. https://doi.org/10.5194/gmd-7-41-2014

Perlwitz, J., Pawson, S., Fogt, R. L., Nielsen, J. E., & Neff, W. D. (2008). Impact of stratospheric ozone hole recovery on Antarctic climate. *Geophysical Research Letters*, *35*, L08714. https://doi.org/10.1029/2008GL033317

Peters, D. H. W., Schneidereit, A., Bügelmayer, M., Zülicke, C., & Kirchner, I. (2015). Atmospheric circulation changes in response to an observed stratospheric zonal ozone anomaly. *Atmosphere-Ocean*, *53*, 74–88. https://doi.org/10.1080/07055900.2013.878833

Polvani, L. M., Waugh, D. W., Correa, G. J., & Son, S. W. (2011). Stratospheric ozone depletion: The main driver of twentieth-century atmospheric circulation changes in the Southern Hemisphere. *Journal of Climate*, *24*(3), 795–812. https://doi.org/10.1175/2010JCLI3772.1

Priestley, A. (1993). A quasi-conservative version of the semi-Lagrangian advection scheme. *Monthly Weather Review*, *121*, 621–629. https://doi.org/10.1175/1520-0493(1993)121<0621:AQCVOT>2.0.CO;2

Ramaswamy, V., Schwarzkopf, M. D., & Randel, W. J. (1996). Fingerprint of ozone depletion in the spatial and temporal pattern of recent lower-stratospheric cooling. *Nature*, *382*(6592), 616–618. https://doi.org/10.1038/382616a0

Roscoe, H. K., Colwell, S. R., & Shanklin, J. D. (2003). Stratospheric temperatures in Antarctic winter: Does the 40-year record confirm midlatitude trends in stratospheric water vapour? *Quarterly Journal of the Royal Meteorological Society*, *129*(591), 1745–1759. https://doi.org/10.1256/qj.02.173

Sassi, F., Boville, B. A., Kinnison, D., & Garcia, R. R. (2005). The effects of interactive ozone chemistry on simulations of the middle atmosphere. *Geophysical Research Letters*, *32*, L07811. https://doi.org/10.1029/2004GL022131

Sheshadri, A., & Plumb, R. A. (2016). Sensitivity of the surface responses of an idealized AGCM to the timing of imposed ozone depletion-like polar stratospheric cooling. *Geophysical Research Letters*, *43*, 2330–2336. https://doi.org/10.1002/2016GL067964

Shine, K. P. (1986). On the modelled thermal response of the Antarctic stratosphere to a depletion of ozone. *Geophysical Research Letters*, *13*, 1331–1334. https://doi.org/10.1029/GL013i012p01331

Silverman, V., Harnik, N., Matthes, K., Lubis, S. W., & Wahl, S. (2017). Radiative effects of ozone waves on the Northern Hemisphere polar vortex and its modulation by the QBO. *Atmospheric Chemistry and Physics Discussions*, 1–33. https://doi.org/10.5194/acp-2017-641

Smith, K. L., & Polvani, L. M. (2014). The surface impacts of Arctic stratospheric ozone anomalies. *Environmental Research Letters*, *9*(7), 074015. http://doi.org/10.1088/1748-9326/9/7/074015

Son, S.-W., Gerber, E. P., Perlwitz, J., Polvani, L. M., Gillett, N. P., Seo, K. H., et al. (2010). Impact of stratospheric ozone on Southern Hemisphere circulation change: A multimodel assessment. *Journal of Geophysical Research*, *115*, D00M07. http://doi.org/10.1029/2010JD014271

Taylor, K. E., Stouffer, R. J., & Meehl, G. A. (2012). An overview of CMIP5 and the experiment design. *Bulletin of the American Meteorological Society*, *93*, 485–498. https://doi.org/10.1175/BAMS-D-11-00094.1

Thompson, D. W., & Solomon, S. (2002). Interpretation of recent Southern Hemisphere climate change. *Science*, *296*(5569), 895–899. http://doi.org/10.1126/science.1069270

Waugh, D., Oman, L., Newman, P., Stolarski, R., Pawson, S., Nielsen, J., & Perlwitz, J. (2009). Effect of zonal asymmetries in stratospheric ozone on simulated Southern Hemisphere climate trends. *Geophysical Research Letters*, *36*, L18701. https://doi.org/10.1029/2009GL040419